Optimal Control Method of Motoring Operation for SRM Drives in Electric Vehicles

X. D. Xue, *Member, IEEE*, K. W. E. Cheng, *Senior Member, IEEE*, J. K. Lin, Z. Zhang, K. F. Luk, T. W. Ng, and N. C. Cheung, *Senior Member, IEEE*

***Abstract*—This paper presents three criteria for evaluating the motoring operations of switched reluctance motor (SRM) drives for electric vehicles (EVs). They imply motoring torque, copper loss, and torque ripple, respectively. The effects of the turn-off and turn-on angles on these criteria are investigated under hysteresis current control. To fulfill the best motoring operation, consequently, the multiobjective optimization function is developed by using three weight factors and three groups of base values: the correct balance between the maximum average torque, the maximum average torque per root mean square current, and the maximum torque smoothness factor. The study in this paper shows that the turn-off and the turn-on angles can be optimized to maximize the developed multiobjective function. In addition, the control method for the best motoring operation of SRM drives in EVs is proposed. In this method, two angular controllers are proposed to automatically tune the turn-off and turn-on angles to obtain high motoring torque, low copper loss, and low torque ripple. Simulations and experimental results have demonstrated the proposed optimal control method. Therefore, this paper offers a valuable and feasible approach for implementing the best motoring operation of SRM drives for EVs.**

***Index Terms*—Control, electric vehicles (EVs), optimization, switched reluctance motor (SRM) drives.**

I. Introduction

DUE to simple and rugged motor construction, low weight, potentially low production cost, undemanding cooling, excellent torque–speed characteristics, high torque density, high operating efficiency, and inherent fault tolerance, switched reluctance motor (SRM) drives are emerging as an attractive solution for electric vehicle (EV) applications [1]–[4]. Traction performances of EVs depend on the performances of SRM drives. Hence, the excellent motoring operation of SRMs is important for EVs with high performances. This paper is focused on this challenging issue.

Manuscript received June 3, 2009; revised September 26, 2009 and December 9, 2009. First published January 22, 2010; current version published March 19, 2010. This work was supported in part by the Innovation and Technology Fund of the Hong Kong Innovation and Technology Support Program and in part by the Automotive Parts and Accessory Systems R&D Centre, Hong Kong, under Project ITF/013/07AP (PolyU code: ZS01). The review of this paper was coordinated by Dr. C. C. Mi.

The authors are with the Department of Electrical Engineering, Hong Kong Polytechnic University, Kowloon, Hong Kong (e-mail: eexdxue@polyu.edu.hk; eeecheng@polyu.edu.hk; linjiongkang@hotmail.com; 09901316r@polyu.edu.hk; eekfluk@polyu.edu.hk; tszwang0408@hotmail.com; norbert.cheung@polyu.edu.hk).

Color versions of one or more of the figures in this paper are available online at http://ieeexplore.ieee.org.

Digital Object Identifier 10.1109/TVT.2010.2041260

Some studies relative to this issue have been reported. Fahimi *et al.* [5] presented an adaptive control scheme to maximize torque per ampere at low and high speeds, and the turn-on and turn-off angles were self-tuned by using artificial neural networks. In [6], a generic algorithm was used to optimize the turn-on and turn-off angles to maximize average torque. In current and voltage control strategies, the turn-off angle was optimized to maximize energy conversion per stroke. Furthermore, the formulas for the optimal turn-off angles were developed in [7]. The turn-on and turn-off angles were optimized to maximize the drive system efficiency and the peak overload capability in [8]. To maximize SRM efficiency, the turn-on angle was optimized, and the conduction angle was maintained at a constant to maximize the ratio of the average torque to root mean square (rms) current [9]. A new method that determines the optimal turn-on and turn-off angles online was proposed in [10] to accomplish an acceptable balance between energy efficiency and torque ripple criteria. Niazi *et al.* [11] proposed the control method to maximize torque per ampere, which was applied to permanent-magnet-assisted synchronous reluctance motors for traction application. A control strategy to minimize the losses of an induction motor propelling an EV was presented in [12]. For those reported techniques, in summary, control objectives were selected to maximize average torque, to maximize torque per rms current, to maximize efficiency, to minimize loss, or to obtain the balance between maximum efficiency and minimum torque ripple.

The aim of this study is to find an optimal control method to implement the best motoring operation of SRM drives in EVs. The best motoring operation is regarded as high motoring torque, high operating efficiency, and low torque ripple. Different from previously reported optimization objectives, the developed multiobjective function is the correct compromise between maximum average torque, maximum average torque per rms current (minimum copper loss), and maximum torque smoothness factor (minimum torque ripple). Thus, the proposed multiobjective function meets the requirement of the best motoring operation of electric motor drives in EVs. Consequently, the turn-off and turn-on angles are optimized by using the proposed multiobjective function. Two angular controllers are proposed to automatically adjust the turn-on and turn-off angles to obtain higher motoring torque, lower copper loss, and lower torque ripple. The simulation and experimental results will demonstrate that the proposed method can be used to implement the best motoring operation of SRM drives in EVs.

II. Characteristics of Motoring Operation of Switched Reluctance Motor Drives

In general, motoring operation of SRM drives can be classified into two modes. One is the constant torque operation at low and medium speeds, and the other is the constant power one at high speed. The in-wheel SRM drive is used to directly drive vehicle wheels in this study. Thus, the motoring operation of the in-wheel SRM drive is regarded as the constant torque operation in this paper. Furthermore, the current hysteresis control is selected to implement the constant torque operation. In this case, the controlled parameters in SRM drives can be selected as the turn-on angle, the turn-off angle, and the current reference.

A. Model of SRM Drives

For SRM drives, the phase flux linkage and phase current must satisfy the following equation:

$$V_{\rm ph} = \frac{d\psi(\theta, i)}{dt} + ir_{\rm ph} \tag{1}$$

where $V_{\rm ph}$ represents the voltage applied to a phase winding, ψ represents the phase flux linkage, θ represents the rotor position, i represents the phase current, t represents the time, and $r_{\rm ph}$ represents the phase resistance.

For the specified SRM drives, the flux linkage and torque characteristics can be obtained by using finite-element analysis or the experiment, which are expressed as

$$\psi(\theta, i) = f_\psi(\theta, i) \tag{2}$$

$$T_{\rm ph}(\theta, i) = f_T(\theta, i) \tag{3}$$

where $T_{\rm ph}$ represents the torque produced by one phase.

Neglecting ON-state drop of power switches, the relationships between the dc-link voltage, phase voltage, turn-on angle, turn-off angle, rotor position, current reference, and phase current can be given as

$$\begin{aligned} V_{\rm ph} &= V_{\rm dc} \quad (i \le I_{\rm ref} - 0.5I_b) \\ V_{\rm ph} &= 0 \quad (i \ge I_{\rm ref} + 0.5I_b) \quad (\theta_{\rm on} \le \theta < \theta_{\rm off}) \end{aligned} \tag{4}$$

$$V_{\rm ph} = -V_{\rm dc} \quad (\theta_{\rm off} \le \theta \le \theta_e) \tag{5}$$

where $V_{\rm dc}$ denotes the dc-link voltage, $I_{\rm ref}$ denotes the current reference, I_b denotes the hysteresis band, $\theta_{\rm on}$ denotes the turn-on angle, $\theta_{\rm off}$ denotes the turn-off angle, and θ_e denotes the extinguishing angle.

B. Criteria for Motoring Operation

From the requirement of EVs on motoring operation of electric motors [4], the following three criteria are proposed: 1) the average torque; 2) the average torque per rms current; and 3) the torque smoothness factor. They imply the magnitudes of motoring torque, the operating efficiency, and the torque ripple, respectively.

The computation of the average torque in SRM drives is given as

$$T_{\rm ave} = \frac{1}{\theta_p} \int_{\theta_{\rm on}}^{(\theta_{\rm on}+\theta_p)} \sum_{k=1}^{N_{\rm ph}} T_{\rm phk}(\theta, i) d\theta \tag{6}$$

where θ_p denotes the period of the phase current, $N_{\rm ph}$ denotes the number of phases, and $T_{\rm phk}$ denotes the phase torque.

Consequently, the average torque per rms current is expressed as

$$TC = \frac{T_{\rm ave}}{I_{\rm rms}} \tag{7}$$

where $I_{\rm rms}$ denotes the rms value of the phase current.

In this paper, the torque smoothness factor is defined as

$$TSF = \min\left\{ \frac{T_{\rm ave}}{T_{\rm max} - T_{\rm ave}}, \frac{T_{\rm ave}}{T_{\rm ave} - T_{\rm min}} \right\} \tag{8}$$

where $T_{\rm max}$ represents the maximum value of instantaneous torque, and $T_{\rm min}$ represents the minimum value of instantaneous torque.

For SRM drives in EVs, the values of the three criteria are desired to be as large as possible because large average torque, large average torque per rms current, and large torque smoothness factor imply high torque, low copper loss (high operating efficiency), and low torque ripple, respectively.

Investigating the effects of the controlled parameters on the criteria is quite helpful in the development of a novel control method for the best motoring operation of SRM drives. In this paper, the prototype of the four-phase, 5-kW, in-wheel SRM drive is used to investigate the optimal control method for motoring operation. The rotor position is defined as 0° when the stator pole is fully unaligned with the rotor pole, and the rotor position is defined as 30° when the stator pole is completely aligned with the rotor pole. The characteristics of the flux linkage of the prototype are illustrated in Fig. 1 and are computed by using the experiment. Hence, the above model can be solved by using the given flux linkage characteristics [13], [14], and consequently, three criteria can be computed.

C. Effects of Current Reference

Fig. 2(a) illustrates the effect of the current reference, and the results in Fig. 2(a) are obtained when the turn-on angle is equal to 0° and the turn-off angle is equal to 22°. At various motor speeds, the following can be observed: 1) The average torque becomes large if the current reference increases; 2) the average torque per rms current goes up if the current reference increases; and 3) the torque smoothness factor increases with an increment in the current reference.

For various turn-off angles, the effect of the current reference is shown in Fig. 2(b) when the SRM is running at a turn-on angle of 0° and a motor speed of 500 r/min. The following can be observed: 1) The large current reference results in the large

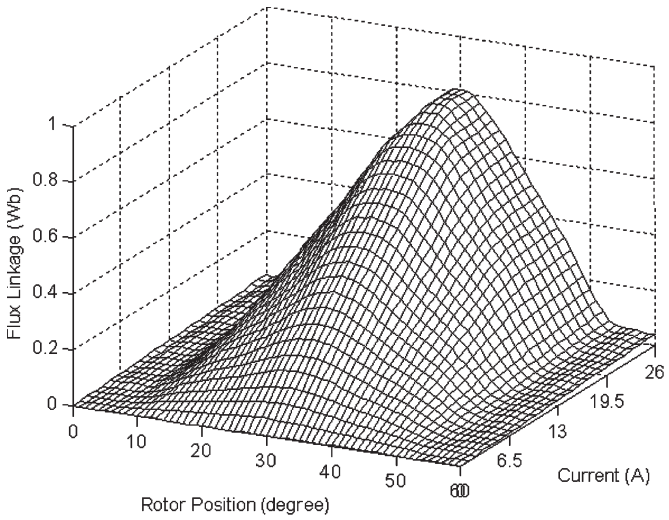

Fig. 1. Given flux linkage characteristics of the prototype.

average torque; 2) the average torque per rms current changes with the current reference; and 3) the torque smoothness factor goes up with increase in the current reference.

For a group of given turn-on angles, Fig. 2(c) depicts the effect of the current reference at a turn-off angle of 24° and a motor speed of 500 r/min. It can be observed that the average torque, the average torque per rms current, and the torque smoothness factor are augmented with an increase in the current reference.

Therefore, Fig. 2 indicates that the large current reference is beneficial for the implementation of the desired motoring operation of SRM drives in EVs.

D. Effects of the Turn-Off Angle

When the SRM is operating at a turn-on angle of 0° and a current reference of 15 A, the changes of the average torque, the average torque per rms current, and the torque smoothness factor with the turn-off angle are depicted in Fig. 3(a). The following can be observed: 1) There are optimal turn-off angles at various motor speeds such that the average torque leads to the maximum values; 2) there are optimal turn-off angles and the maximum average torque per rms current for different motor speeds; and 3) the optimal turn-off angles can be found at various motor speeds to obtain the maximum torque smoothness factors.

Fig. 3(b) shows the effect of the turn-off angle at various current references when the SRM is running at a motor speed of 500 r/min and a turn-on angle of 0°. The following can be observed: 1) The optimal turn-off angles can be determined at various current references to maximize the average torque; 2) the optimal turn-off angles at different current references can be found to achieve the maximum values of the average torque per rms current; and 3) there are optimal turn-off angles at various current references to obtain the maximum torque smoothness factors.

The effect of the turn-off angle at various turn-on angles is illustrated in Fig. 3(c) when the SRM is working at a motor speed of 500 r/min and a current reference of 15 A. The following can be observed: 1) There are optimal turn-off angles

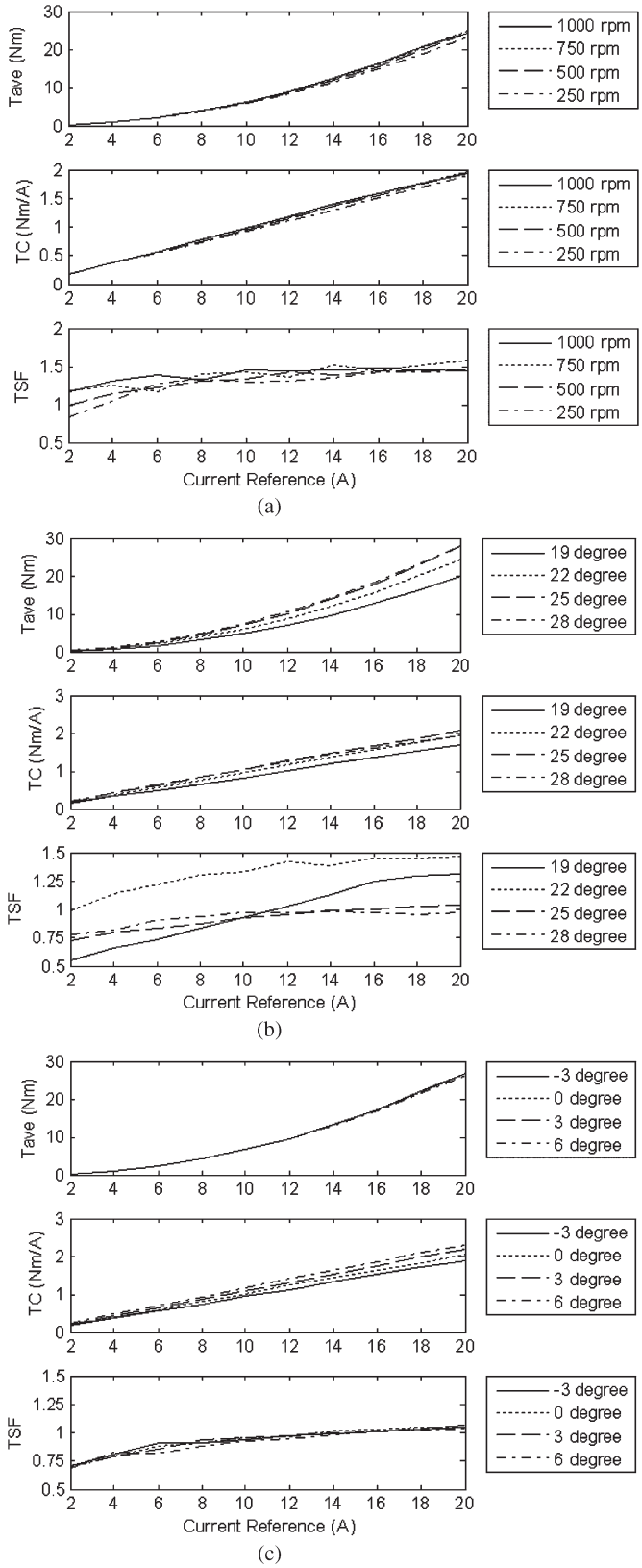

Fig. 2. Effects of the current reference. (a) Various motor speeds. (b) Various turn-off angles. (c) Various turn-on angles.

to maximize the average torque; 2) the maximum values of the average torque per rms current can be obtained when the turn-off angles are equal to the optimal values, and 3) there are

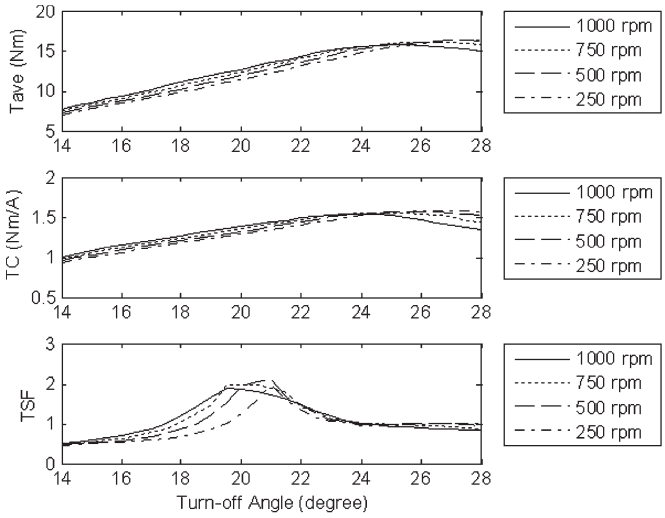

Fig. 3. Effects of the turn-off angle. (a) Various motor speeds. (b) Various current references. (c) Various turn-on angles.

always optimal turn-off angles such that the torque smoothness factor reaches the maximum values.

As a result, the turn-off angle has significant effects on the motoring operation of SRM drives. The turn-off angle can be optimized to obtain the maximum average torque, the maximum average torque per rms current, or the maximum torque smoothness factor.

E. Effects of the Turn-On Angle

Fig. 4(a) illustrates the effect of the turn-on angle at various motor speeds when the SRM is running at a turn-off angle of 24° and a current reference of 15 A. The following can be observed: 1) The average torque has similar values if the turn-on angle is smaller than 6°, and the average torque goes down with an increase in the turn-on angle if the turn-on angle is larger than 6°; 2) there are optimal turn-on angles such that the average torque per rms current reaches the maximum values; and 3) the optimal turn-on angles can be found to obtain the maximum torque smoothness factors.

The effect of the turn-on angle at various current references is depicted in Fig. 4(b) when the SRM is working at a motor speed of 500 r/min and a turn-off angle of 24°. The following can clearly be observed: 1) The average torque has similar values if the turn-on angle is smaller than 6°, and the average torque becomes small with an increase in the turn-on angle if the turn-on angle is larger than 6°; 2) the average torque per rms current leads to the maximum value if the turn-on angle is the optimal value; and 3) the optimal turn-on angles can be determined to have the maximum torque smoothness factors.

At various turn-off angles, the effect of the turn-on angle is illustrated in Fig. 4(c) when the SRM is operating at a motor speed of 500 r/min and a current reference of 15 A. The following can be observed: 1) The average torque has similar values if the turn-on angle is smaller than 6°, and the average torque becomes small with an increase in the turn-on angle if the turn-on angle is larger than 6°; 2) there are optimal turn-on angles to obtain the maximum values of the average torque per rms current; and 3) the optimal turn-on angles can be found to maximize the torque smoothness factor.

Therefore, the turn-on angle has considerable effects on the motoring operation of SRM drives. Optimal turn-on angles can be found to maximize the average torque, the average torque per rms current, or the torque smoothness factor.

III. Optimization of the Single-Objective Function

A. Optimization Function With a Single Objective

The discussion in Section II shows that the reference current, the turn-on angle, and the turn-off angle can be used to control the torque, torque per ampere, and torque ripple of the motor. To achieve the proposed optimization objective, a direct solution is to optimize the current reference, the turn-on angle, and the turn-off angle at various motor speeds. However, such an optimization with three variables will result in complicated computations. Considering flexible control modes of SRM drives, an alternative solution is developed in this paper to simplify the optimization computation. The proposed solution is that the turn-on and turn-off angles are optimized at various current references and motor speeds to achieve the same optimization objective. In actual application, consequently, the optimal turn-on and turn-off angles can be determined from the actual current reference and motor speed.

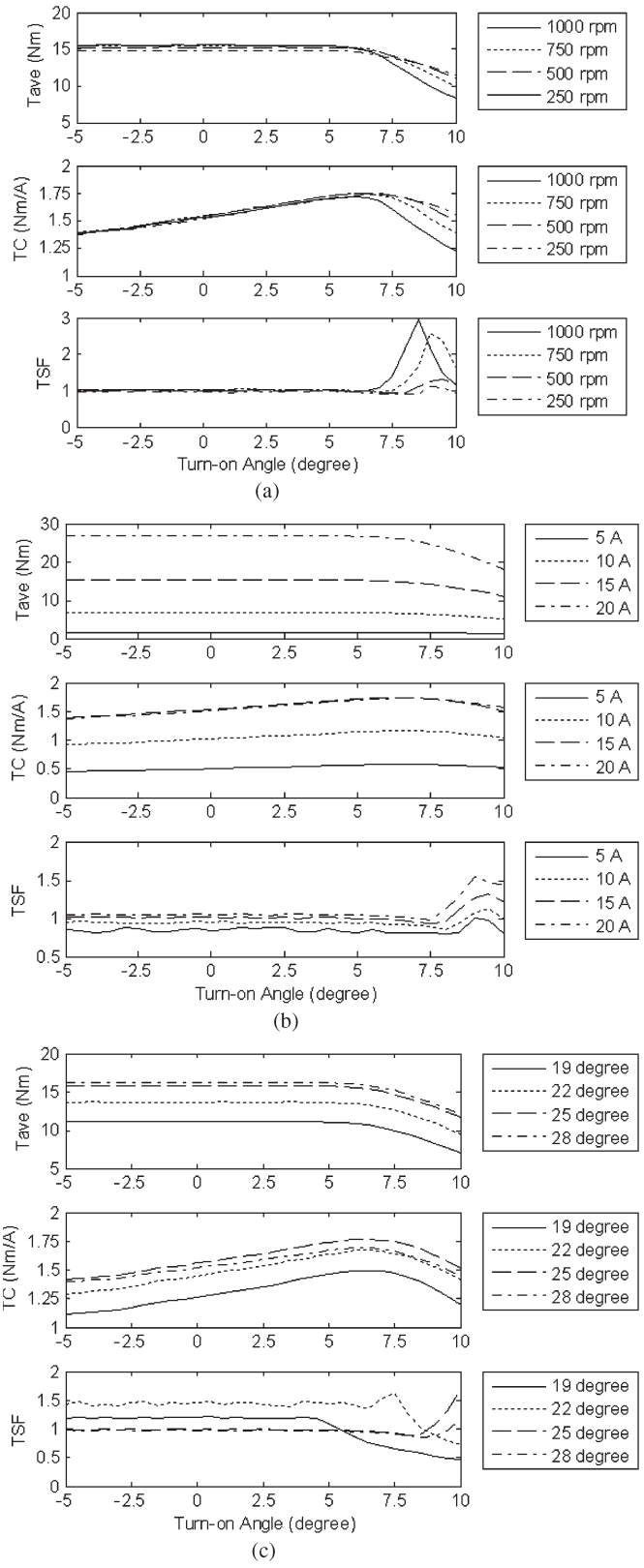

Fig. 4. Effects of the turn-on angle. (a) Various motor speeds. (b) Various current references. (c) Various turn-off angles.

The total losses in the motor should be considered for the optimization. The total losses mainly include the copper and iron losses. For a specified motor, the iron loss depends on the flux density and the flux frequency. In this paper, the optimization is carried out at a specified current reference and at a specified motor speed. Hence, the dc-link voltage, the current reference, and the motor speed are all constant when optimizing the turn-on and turn-off angles. Consequently, the iron loss during the optimization changes a little. It can be seen that variation in the total losses is mainly dependent on the one in the copper loss during the optimization. In this paper, therefore, the copper loss is only taken into account during the optimization.

From the discussion in Section II, it can be concluded that at any current reference and motor speed, the optimal turn-on and turn-off angles can be found to maximize the average torque, the average torque per rms current, or the torque smoothness factor. Apparently, the optimization function will include only one objective. In this section, hence, the turn-on and turn-off angles will be optimized for three different optimization functions, which are the average torque, the average torque per rms current, and the torque smoothness factor.

These three optimization objective functions can be defined, respectively, as follows:

$$F_t\left(\theta_{\rm on}^{\rm opt},\theta_{\rm off}^{\rm opt}\right)=\max\{T_{\rm ave}\} \tag{9}$$

$$F_{tc}\left(\theta_{\rm on}^{\rm opt},\theta_{\rm off}^{\rm opt}\right)=\max\{TC\} \tag{10}$$

$$F_{\rm tsf}\left(\theta_{\rm on}^{\rm opt},\theta_{\rm off}^{\rm opt}\right)=\max\{TSF\} \tag{11}$$

where F_t denotes the optimization function of the average torque, F_{tc} denotes the optimization function of the average torque per rms current, $F_{\rm tsf}$ denotes the optimization function of the torque smoothness factor, $\theta_{\rm on}^{\rm opt}$ denotes the optimal turn-on angle, and $\theta_{\rm off}^{\rm opt}$ denotes the optimal turn-off angle.

The developed 2-D search algorithm is used to optimize the turn-on and turn-off angles. For the prototype of the four-phase SRM drive, the turn-on angle changes in the range from -5° to 10°, the turn-off angle varies in the range from 14° to 28°, and the conduction angle must not be larger than 30°. The step size to search for the optimal turn-on and turn-off angles is selected as 0.5°.

B. Optimization Results to Maximize the Average Torque

Fig. 5 illustrates the optimization results for maximization of the average torque. Fig. 5(a) shows the distribution of the optimal turn-on angles. The optimal turn-on angle changes in the range from 0° to 4.5°. The average value of the optimal turn-on angles is calculated as 1.875°. Fig. 5(b) illustrates the distribution of the optimal turn-off angles. It can be observed that the optimal turn-off angle changes in the range from 24.5° to 28°. The average value of the optimal turn-off angles is equal to 27.094°. In addition, the maximum values of the average torque are depicted in Fig. 5(c).

C. Optimization Results to Maximize the Average Torque per RMS Current

The optimization results for maximization of the average torque per rms current are shown in Fig. 6. The optimal turn-on angles for maximizing average torque per rms current can be observed in Fig. 6(a). The maximum value of the optimal turn-on angles is 6.5°, and the minimum value is 5.5°. The average value of the optimal turn-on angles is equal to 6.313°. The distribution of the optimal turn-off angles for maximizing

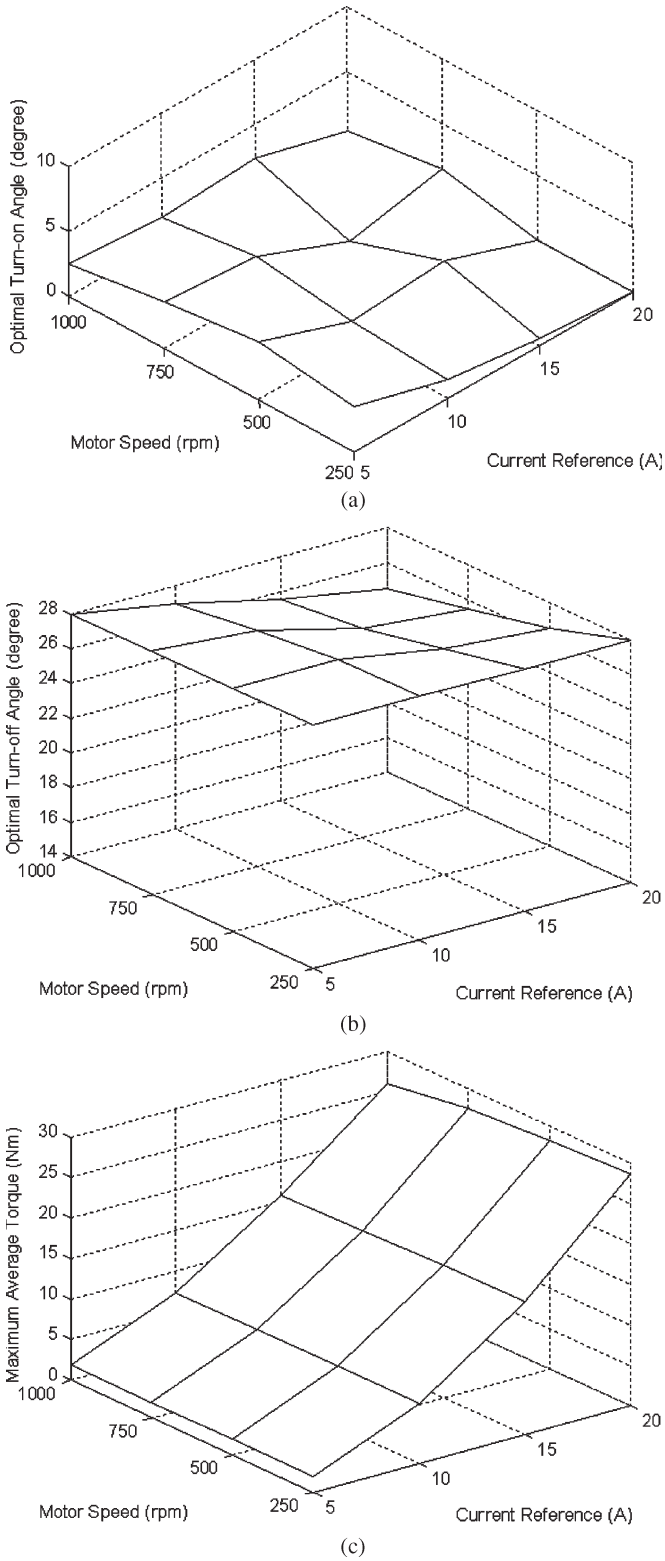

Fig. 5. Maximization of average torque. (a) Optimal turn-on angle. (b) Optimal turn-off angle. (c) Maximum average torque.

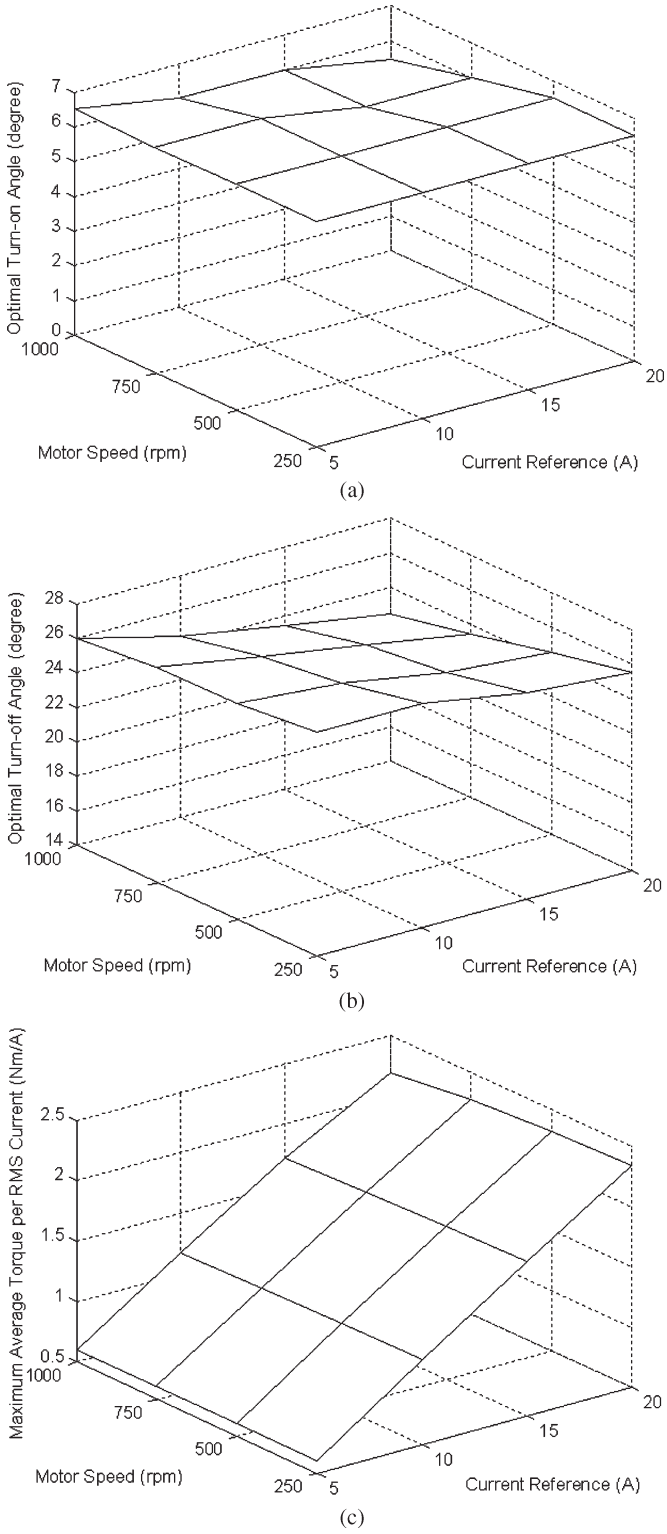

Fig. 6. Maximization of the average torque per rms current. (a) Optimal turn-on angle. (b) Optimal turn-off angle. (c) Maximum value of average torque per rms current.

average torque per rms current is shown in Fig. 6(b). The optimal turn-off angle varies in the range from 22.5° to 27.0° and the average value of the optimal turn-off angles for the maximum average torque per rms current is 25.25°. Furthermore, Fig. 6(c) illustrates the maximum values of the average torque per rms current.

D. Optimization Results to Maximize the Torque Smoothness Factor

Fig. 7 shows the optimization results for maximizing the torque smoothness factor. The optimal turn-on angles for maximizing the torque smoothness factor are illustrated in Fig. 7(a).

They vary in the range from 0.5° to 10°. The average value of the optimal turn-on angles is 7.125°. Fig. 7(b) depicts the optimal turn-off angles for maximization of the torque smoothness factor. The maximum value of the optimal turn-off angles is 26.5°, and the minimum value is 21°. The average value of the optimal turn-off angles is computed as 22.5°. Moreover, Fig. 7(c) shows the maximum torque smoothness factors.

IV. Optimization of the Multiobjective Function

A. Optimization Function With Multiple Objectives

The best motoring operation of SRM drives in EVs is to accomplish high torque, low copper loss, and low torque ripple. However, it can be observed from Section III that the turn-on and turn-off angles have different optimal values, respectively, to maximize the average torque, the average torque per rms current, or the torque smoothness factor. In other words, it is impossible to simultaneously maximize those three objectives. It can be seen that maximization of the first objective indicates the maximum motoring torque, maximization of the second one implies the minimum copper loss, and maximization of the third one means the minimum torque ripple. In this paper, thus, the multiobjective function is proposed, and it is defined as the correct compromise between the average torque, the average torque per rms current, and the torque smoothness factor by using three weight factors and three groups of base values. Such a multiobjective function can be expressed as

$$F_{\rm obj} = w_T \frac{T_{\rm ave}}{T_b} + w_{TC} \frac{TC}{TC_b} + w_{TSF} \frac{TSF}{TSF_b} \tag{12}$$

$$w_T + w_{TC} + w_{TSF} = 1 \tag{13}$$

$$T_b = \max\{T_{\rm ave}\} \tag{14}$$

$$TC_b = \max\{TC\} \tag{15}$$

$$TSF_b = \max\{TSF\} \tag{16}$$

where $F_{\rm obj}$ denotes the developed multiobjective function, w_T denotes the weight factor of the average torque, w_{TC} denotes the weight factor of the average torque per rms current, w_{TSF} is the weight factor of the torque smoothness factor, T_b denotes the base value of the average torque, TC_b denotes the base value of the average torque per rms current, and TSF_b denotes the base value of the torque smoothness factor. Those base values have been determined in Section III.

It is clear that the developed multiobjective function includes three criteria for the best motoring operation of SRM drives in EVs. w_T, w_{TC}, and w_{TSF} indicate the expected shares of the average torque, the average torque per rms current, and the torque smoothness factor, respectively. Thus, the optimization function with multiple objectives can be given as

$$F_{\rm opt}\left(\theta_{\rm on}^{\rm opt}, \theta_{\rm off}^{\rm opt}\right) = \max\left\{ w_T \frac{T_{\rm ave}}{T_b} + w_{TC} \frac{TC}{TC_b} + w_{TSF} \frac{TSF}{TSF_b} \right\}. \tag{17}$$

In this paper, the in-wheel SRM drive is applied to EVs, and hence, the importance of the torque or efficiency is stronger than that of the torque smoothness factor. Consequently, it is suggested that the weight factor of the average torque is 0.4, the weight factor of the average torque per rms current is equal

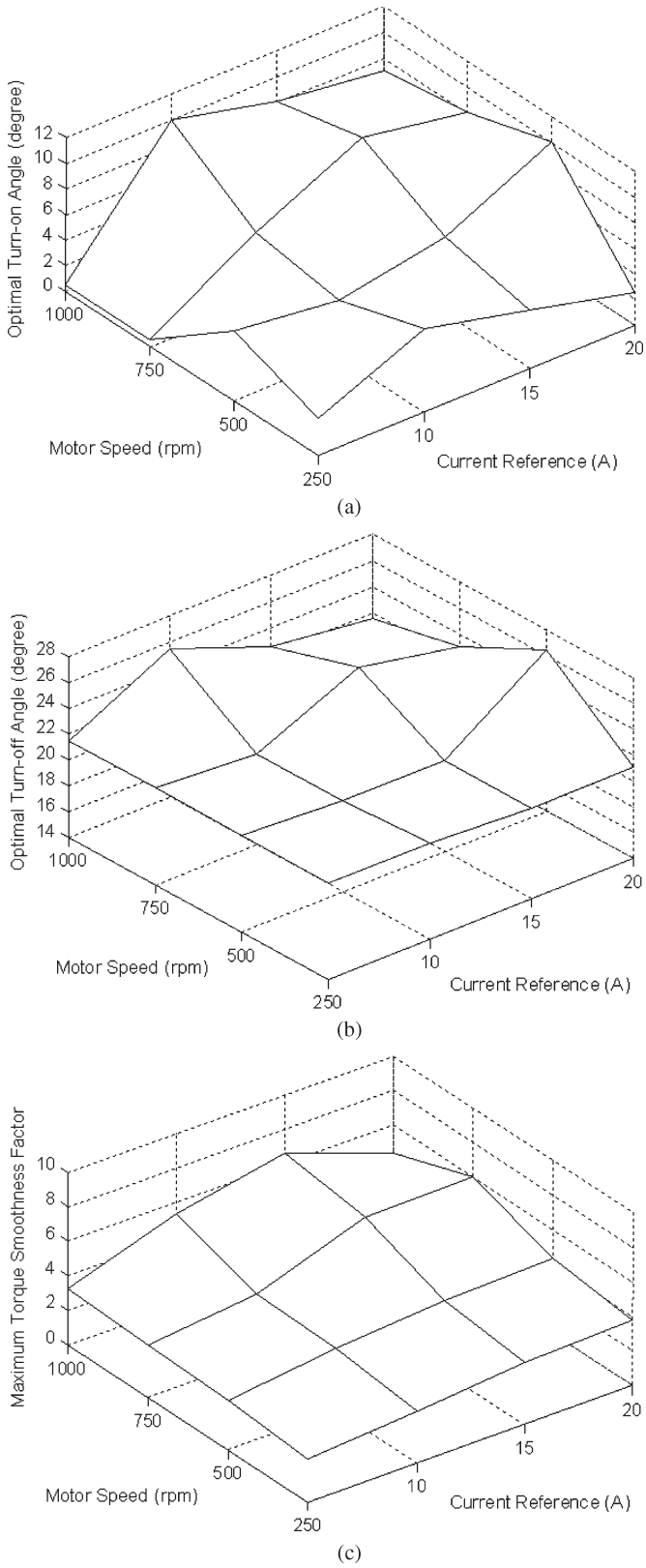

Fig. 7. Maximization of torque smoothness factor. (a) Optimal turn-on angle. (b) Optimal turn-off angle. (c) Maximum torque smoothness factor.

to 0.4, and the weight factor of the torque smoothness factor is equal to 0.2.

B. Optimization Results Under the Best Motoring Operation

Fig. 8 illustrates the optimization results by using the developed multiobjective optimization function. Fig. 8(a) depicts the optimal turn-on angles, which change in the range from 5.5° to 6.5°. The average value of the optimal turn-on angles is calculated as 5.5°. Fig. 8(b) shows the distribution of the optimal turn-off angles, which change in the range from 21.5° to 28°. The average value of the optimal turn-off angles is equal to 25.875°. The maximum values of the developed multiobjective function are given in Fig. 8(c).

V. Control Method of the Best Motoring Operation for Switched Reluctance Motor Drives in Electric Vehicles

A. Optimal Control Method

From the above investigations, the optimal control method to accomplish best motoring operation of the SRM drive for EVs can be proposed as follows.

1) Using the proposed single-objective functions, which are the average torque, the average torque per rms current, and the torque smoothness factor, the turn-off and turn-on angles are optimized at given motor speeds and current references.
2) Based on the developed multiobjective optimization function, which is defined as the correct balance between the average torque, the average torque per rms current, and the torque smoothness factor, the turn-off and turn-on angles are optimized at given motor speeds and current references.
3) The controller models of the turn-off and turn-on angles are defined as the 2-D functions of the motor speed and current reference, respectively.
4) The optimal turn-off and turn-on angles are calculated automatically according to the motor speed and current reference by using the turn-on and turn-off angle controllers.
5) The magnitude of the average motoring torque is adjusted by controlling the current reference.

Fig. 9(a) depicts the flowchart for solving the optimization problem, Fig. 9(b) illustrates the block diagram to optimize the turn-off and turn-on angles for the best motoring operation of SRM drives, and Fig. 9(c) shows the control scheme to implement the proposed optimal control method.

The realization of the proposed control method can be summarized as follows. Referring to Fig. 9(c), first, the proportional–integral speed controller gives the current reference according to the specified speed reference. Based on the current reference and the estimated motor speed, the turn-on and turn-off angle controllers generate the optimal turn-on and turn-off angles, respectively; at the same time, the hysteresis current controller outputs the pulsewidth modulation (PWM) control signals from the current reference, the measured actual current, and the measured rotor position. Finally, the PWM control signals are used to drive the SRM converter circuit.

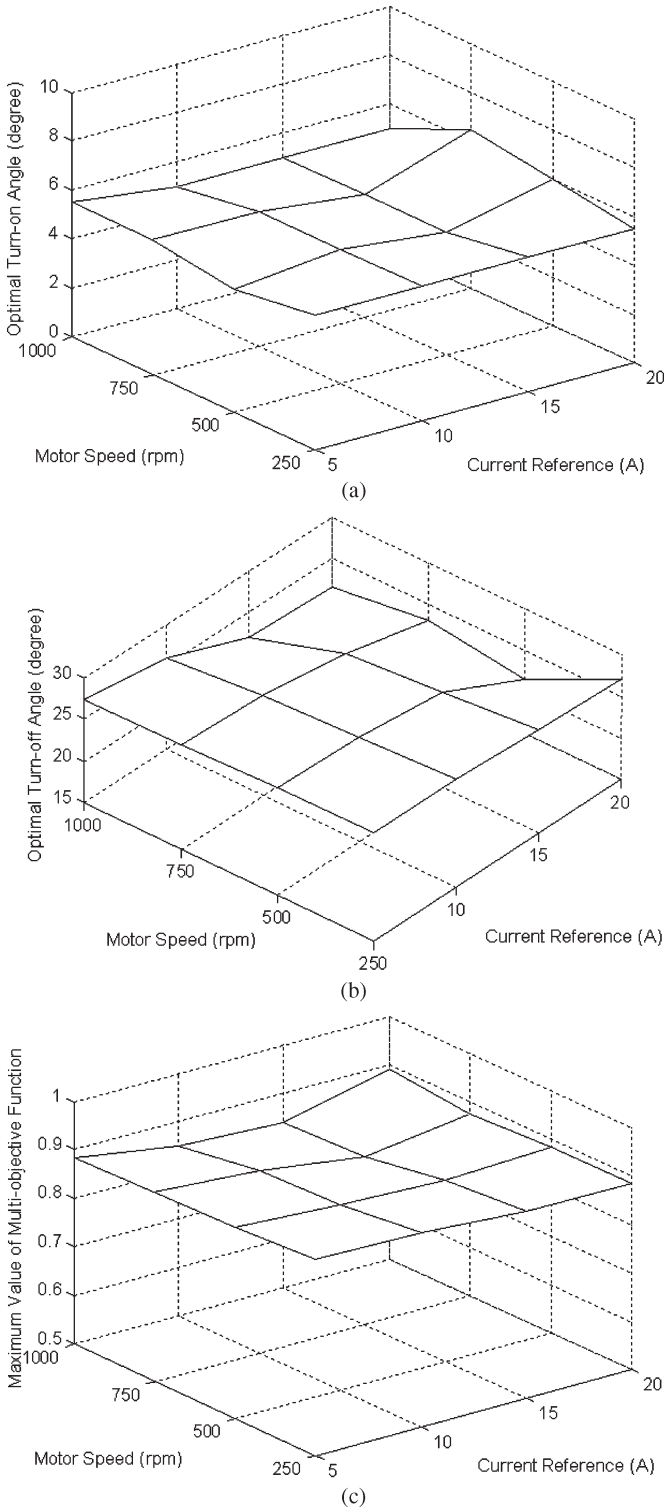

Fig. 8. Maximization of the multiobjective function for best motoring operation. (a) Optimal turn-on angle. (b) Optimal turn-off angle. (c) Multiobjective optimization function.

B. Controllers of Optimal Turn-Off and Turn-On Angles

It can be seen from the discussions in Section IV that the optimal turn-off and turn-on angles depend on the current and motor speed. It should be pointed out that the optimal turn-on angle varies in a small range. Thus, the optimal turn-on angle for the best motoring operation can be determined

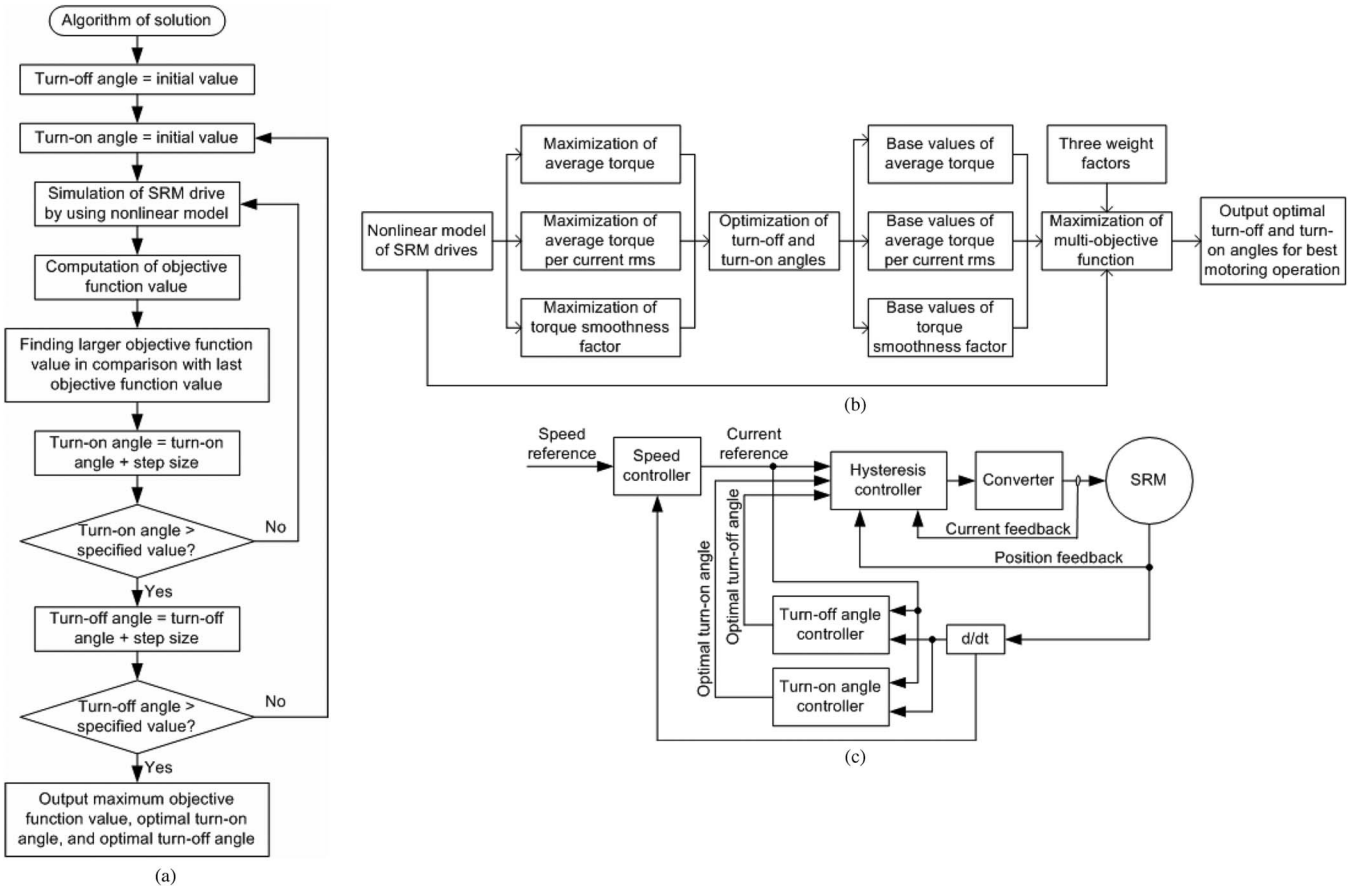

Fig. 9. Schematic diagrams of the proposed optimal control method. (a) Flowchart for solving the optimization problem. (b) Block diagram of the proposed optimization. (c) Schematic diagram of the proposed optimal control.

as the constant value that is equal to 5.5° in this study. As for the optimal turn-off angles, the controller model can be defined by using the 2-D interpolation [14] or the 2-D analytical expressions [15], [16]. In this paper, the controller model of the optimal turn-off angles is expressed as [16]

$$\theta_{\rm off}^{\rm opt}(I_{\rm ref},\omega_r)=\sum_{k=0}^{3}\sum_{j=0}^{3}c_{kj}(I_{\rm ref}-I_{\rm ave})^k(\omega_r-\omega_{\rm ave})^j \quad (18)$$

$$I_{\rm ave}=\sum_{k=0}^{M-1}I_k/M$$

$$\omega_{\rm ave}=\sum_{k=0}^{N-1}\omega_k/N \quad (19)$$

where $\theta_{\rm off}^{\rm opt}$ represents the optimal turn-off angle, $I_{\rm ref}$ represents the current reference, ω_r represents the motor speed, I_k represents the given current reference, M is the number of the given current references, ω_k represents the given motor speed, N is the number of the given motor speeds, and c_{kj} is the least square coefficients that are described in Table I.

Fig. 10 illustrates the comparisons between the computed optimal turn-off angles and the given optimal turn-off angles. From the top to bottom graphs in Fig. 10(a), the current reference is 5, 10, 15, and 20 A, respectively. From the top to bottom graphs in Fig. 10(b), the motor speed is 250, 500, 750, and 1000 r/min, respectively. It can be seen that the developed controller model of the optimal turn-off angle can be used to accurately compute the optimal turn-off angle at real time.

TABLE I
COEFFICIENTS IN THE CONTROLLER MODEL OF THE OPTIMAL TURN-OFF ANGLE

k/j	0	1	2	3
0	.267788E+02	-.251945E+00	-.239924E-01	-.964286E-03
1	-.344901E-02	-.419605E-03	.154124E-04	.548016E-05
2	-.638625E-05	-.108776E-05	.171285E-06	.275630E-07
3	-.115266E-07	-.307064E-08	-.411499E-10	.349150E-11

C. Simulation Verification

Fig. 11 illustrates the simulation results only when maximizing the average torque, which means that the SRM drive runs under the maximum torque control. Hence, $T_{\rm ave}/T_b$ is equal to unity. At the same time, TC/TC_b varies in the range from 0.873 to 0.964, and TSF/TSF_b changes in the range from 0.246 to 0.563. It is clear that the optimal turn-on and turn-off angles for the maximum average torque can accomplish the motoring operation with the maximum average torque. However, the operating efficiency is not high, while the torque ripple is considerably high.

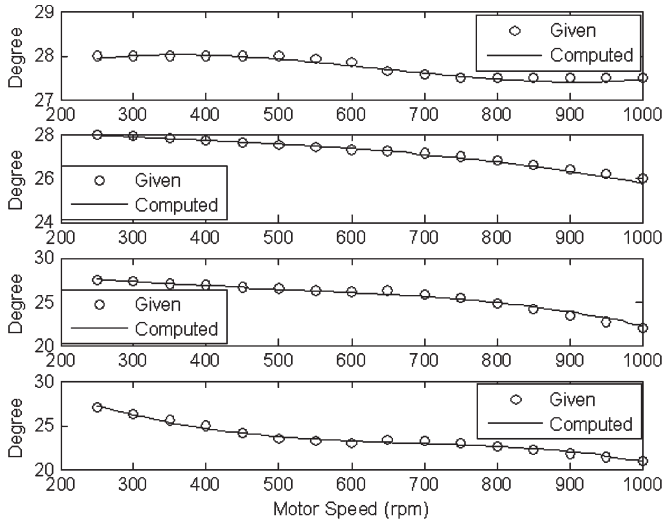

(a)

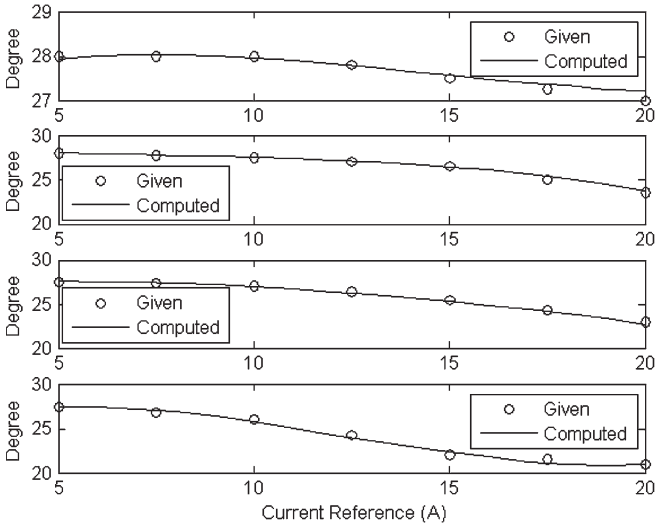

(b)

Fig. 10. Computed and given optimal turn-off angles. (a) Optimal turn-off angle versus motor speed. (b) Optimal turn-off angle versus current reference.

If the optimization objective function is only composed of maximization of the average torque per rms current, the performances of the motoring operation are depicted in Fig. 12. It can be observed that TC/TC_b is always equal to unity, $T_{\rm ave}/T_b$ changes in the range from 0.941 to 0.965, and TSF/TSF_b changes in the range from 0.263 to 0.522. Obviously, the torque ripple is high, although the operating efficiency is considerably high.

In Fig. 13, maximization of the torque smoothness factor is only selected as the optimization objective function. It can be seen that TSF/TSF_b is always equal to unity; however, $T_{\rm ave}/T_b$ is larger than 0.679 and is smaller than 0.770, and TC/TC_b varies in the range from 0.765 to 0.911. It is obvious that the torque ripple is low, but the average torque and operating efficiency are not high.

The above results testify to the fact that the optimization of the single objective gives rise to the maximization of the corresponding individual objective, and other objectives do not have the expected values.

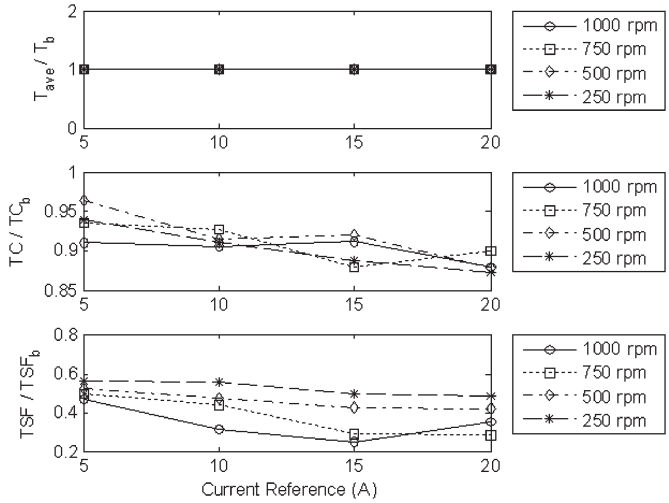

Fig. 11. Motoring operation with maximum average torque.

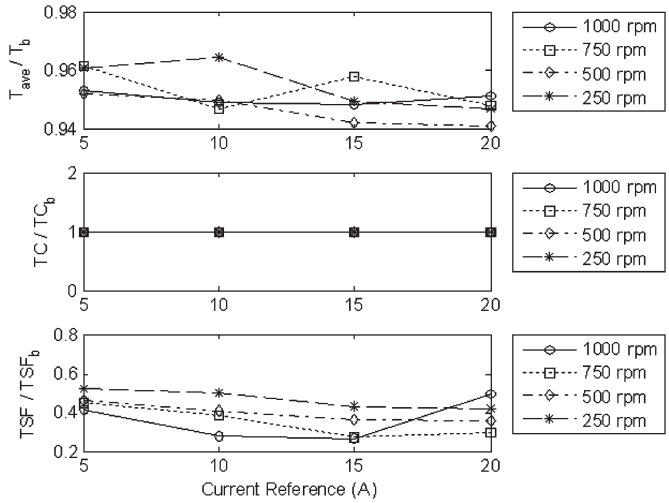

Fig. 12. Motoring operation with maximum average torque per rms current.

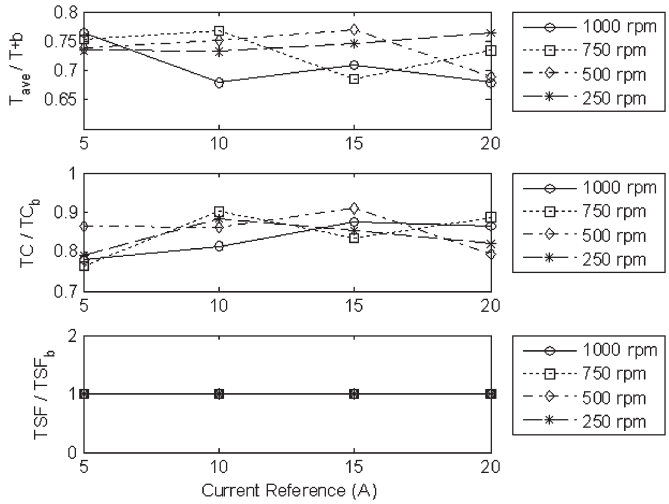

Fig. 13. Motoring operation with maximum torque smoothness factor.

The performances of the best motoring operation are illustrated in Fig. 14, where the compromise between three objectives is selected as the optimization objective function

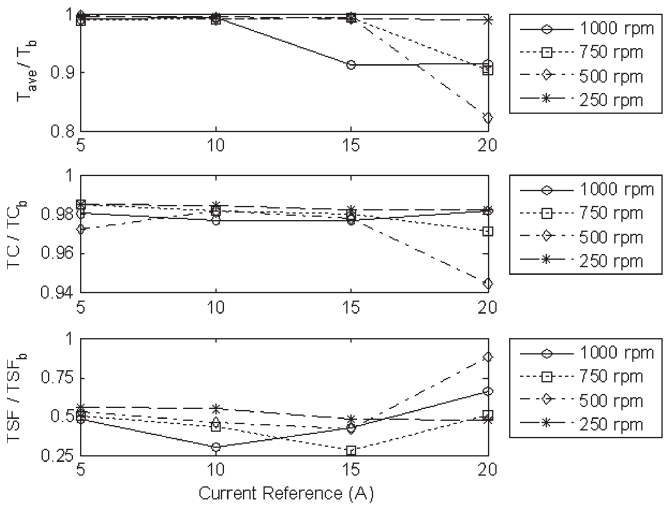

Fig. 14. Best motoring operation.

TABLE II
COMPARISONS BETWEEN FOUR MOTORING OPERATIONS

Average value	I	II	III	IV
T_{ave}/T_b	1	0.951	0.731	0.967
TC/TC_b	0.909	1	0.845	0.978
TSF/TSF_b	0.425	0.395	1	0.498

($w_t = w_{tc} = 0.4$, and $w_{\text{tsf}} = 0.2$). It can be observed that T_{ave}/T_b is larger than 0.822 and smaller than 0.998, TC/TC_b changes in the range from 0.945 to 0.986, and TSF/TSF_b changes in the range from 0.284 to 0.883.

Table II shows the comparisons of the average values of three objectives. Operation I maximizes the average torque, operation II maximizes the average torque per rms current, operation III maximizes the torque smoothness factor, and operation IV maximizes the multiple objectives. It can be seen that the optimal turn-off and turn-on angles under the best motoring operation result in the large T_{ave}/T_b, TC/TC_b, and TSF/TSF_b, which indicate high average torque, low copper loss, and low torque ripple, respectively. Clearly, the proposed optimal control method meets the requirements of the best motoring operation of SRM drives for EVs.

D. Experimental Verification

The experimental setup of the prototype is depicted in Fig. 15. Fig. 16 shows the simulated and experimental current waveforms when the in-wheel SRM drive runs at a speed of 752 r/min. The measured output torque is 7 N · m, and the predicted average output torque is 7.368 N · m. The predicted torque smoothness factor is equal to 1.831. The agreements between the simulated and measured current waveforms indicate that the simulation model and simulation results are accurate.

Figs. 17 and 18 illustrate the experimental comparisons between the proposed optimal motoring control and the traditional motoring control with the constant turn-on and turn-off angles. For the same output torque, it can be observed that the phase rms current under the proposed optimal motoring control is smaller than the one under the traditional motoring control and that the average torque per rms current (TC) under the proposed optimal motoring control is larger than the one under the traditional motoring control. It shows that the proposed optimal motoring control results in smaller copper loss and larger output torque than the traditional motoring control.

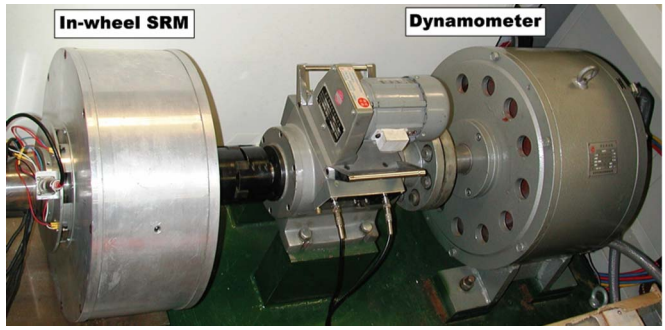

Fig. 15. Experimental setup of the prototype.

(a)

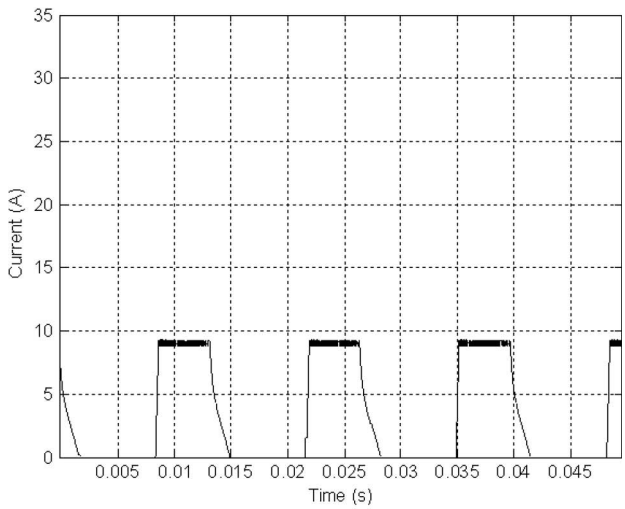

(b)

Fig. 16. Current waveforms. (a) Measured current waveforms (horizontal unit: 5 ms/div; vertical unit: 5 A/div). (b) Simulated current waveforms.

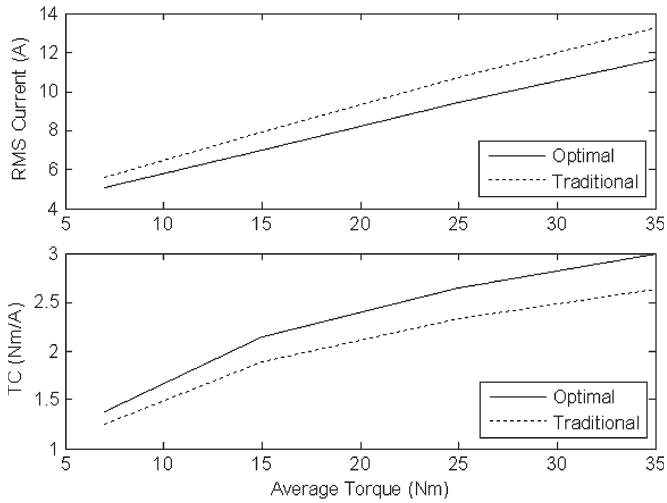

Fig. 17. Experimental results at a motor speed of 200 r/min.

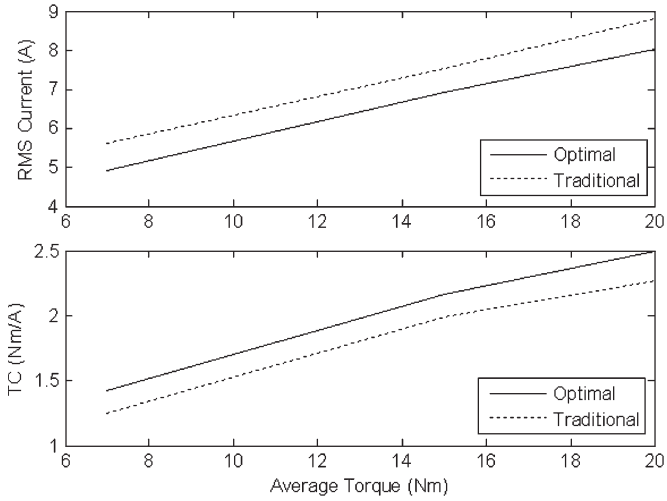

Fig. 18. Experimental results at a motor speed of 500 r/min.

TABLE III
PERFORMANCES IMPROVED BY THE PROPOSED OPTIMAL METHOD

Motor speed (rpm)	Torque (Nm)	Variation in TC	Variation in square of rms current
200	7	10.995%	-18.936%
	15	14.028%	-23.08%
	25	13.271%	-22.0%
	35	13.64%	-22.613%
500	7	14.022%	-23.086%
	15	8.497%	-15.038%
	20	9.868%	-17.13%

In comparison with the results under the traditional control, Table III describes the decreasing percent of the square of the rms current and the increasing percentage of the average torque per rms current under the proposed optimal motoring control.

Clearly, the average torque per rms current (TC) is the capacity that the current produces the torque, and the square of the rms current implies the copper loss. Thus, the proposed optimal control method can result in a larger average torque that is increased by over 10% at 200 r/min, in comparison with the traditional control method. Furthermore, the copper loss can be reduced by over 15%. In other words, the proposed optimal control method can improve the dynamic and steady-state performances of EVs and extend the service life of the battery in EVs. In summary, the experimental results demonstrate that the proposed optimal control method can achieve the best motoring operation of SRM drives for EVs.

Fig. 19. EV prototype with two in-wheel SRM drives.

The proposed control method for the best motoring operation of SRM drives has been applied to an EV prototype, in which two in-wheel SRMs are integrated with two rear rims and, hence, drive two rear wheels directly, respectively, as shown in Fig. 19. The EV prototype has run successfully.

E. Comparisons With Reported Optimization Methods

For SRM drives in EVs, the typical optimization methods published include the maximization of torque and the maximization of torque per ampere. Figs. 20 and 21 show the comparisons between the proposed method and published methods at a current reference of 10 A.

Fig. 20 illustrates the comparisons between the proposed method and the reported method to maximize torque. It can be seen that the torque and torque smoothness factor from the proposed method are approximately consistent with the torque and torque smoothness factor from the reported method, respectively. However, the torque per rms current from the proposed method is much larger than the one from the reported method. Therefore, the proposed method is better than the reported method to maximize torque.

The comparisons between the proposed method and the method to maximize torque per ampere are shown in Fig. 21. It can be observed that the torque per rms current from the proposed method and the one from the reported method are much the same. However, the torque and the torque smoothness factor from the proposed method are larger than the torque and the torque smoothness factor from the reported method, respectively. This indicates that the proposed method is better than the reported method to maximize torque per ampere.

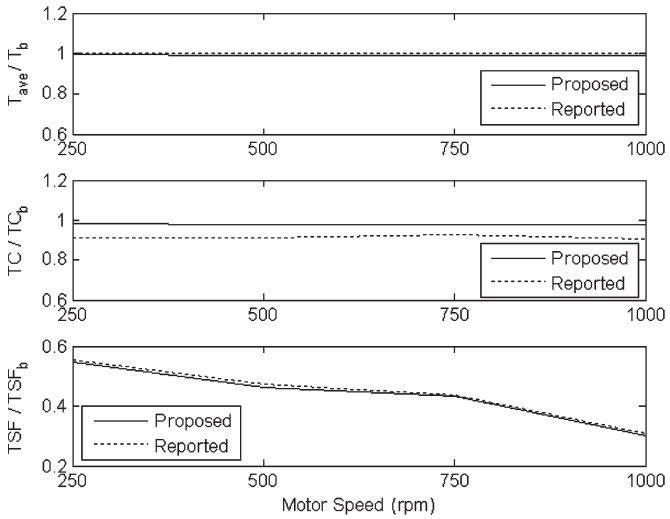

Fig. 20. Comparisons between the proposed method and the reported method for maximizing torque.

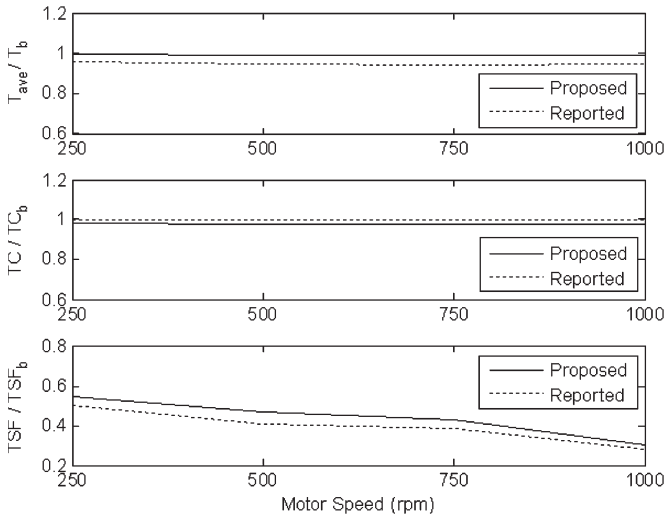

Fig. 21. Comparisons between the proposed method and the reported method for maximizing torque per ampere.

Therefore, the above discussion shows that the proposed method is better than reported methods due to roundly considering requirements of EVs on SRM drives.

VI. Conclusion

In this paper, three criteria have been proposed to evaluate the motoring operation of SRM drives in EVs. They are the average torque, the average torque per rms current, and the torque smoothness factor. These three criteria imply the motoring torque, copper loss, and torque ripple, respectively. The investigation on the motoring operation of the in-wheel SRM drive has shown that the turn-on and turn-off angles have considerable effects on the three criteria and that the turn-on and turn-off angles can be optimized to obtain maximum average torque, maximum average torque per rms current, or maximum torque smoothness factor.

By using three weight factors and three groups of base values, the optimization function with multiple objectives has been developed. It is defined as the compromise between the average torque, the average torque per rms current, and the torque smoothness factor. The optimized variables are selected as the turn-on and turn-off angles. The proposed multiobjective optimization function matches the best motoring operation of SRM drives for EVs. Best motoring operation means high motoring torque, high operating efficiency, and low torque ripple in this paper.

The optimal control method for the best motoring operation of SRM drives in EVs has been proposed. It is based on the developed multiobjective optimization model. This method can accomplish high torque, high operating efficiency, and low torque ripple. The simulation and experimental results have demonstrated that the proposed optimal control method can be used to improve the dynamic and steady-state performances and operating efficiency and, hence, to extend the service life of the battery in EVs. Therefore, this paper provides a feasible and valuable control method to improve performances of in-wheel SRM drives for EVs.

Acknowledgment

The authors would like to thank W. W. Chan and C. Y. Lam for their support with mechanical fixing.

References

[1] C. S. Edrington, M. Krishnamurthy, and B. Fahimi, "Bipolar switched reluctance machines: A novel solution for automotive applications," *IEEE Trans. Veh. Technol.*, vol. 54, no. 3, pp. 795–808, May 2005.

[2] M. Zeraoulia, M. E. H. Benbouzid, and D. Diallo, "Electric motor drive selection issues for HEV propulsion systems: A comparative study," *IEEE Trans. Veh. Technol.*, vol. 55, no. 6, pp. 1756–1764, Nov. 2006.

[3] H.-C. Chang and C.-M. Liaw, "Development of a compact switched-reluctance motor drive for EV propulsion with voltage-boosting and PFC charging capabilities," *IEEE Trans. Veh. Technol.*, vol. 58, no. 7, pp. 3198–3215, Sep. 2009.

[4] X. D. Xue, K. W. E. Cheng, and N. Cheung, "Selection of electric motor drives for electric vehicles," presented at the Australasian Universities Power Engineering Conf., Sydney, Australia, 2008.

[5] B. Fahimi, G. Suresh, J. P. Johnson, M. Ehsani, M. Arefeen, and I. Panahi, "Self-tuning control of switched reluctance motors for optimized torque per ampere at all operating points," in *Proc. 13th Annu. Appl. Power Electron. Conf. Expo.*, 1998, vol. 2, pp. 778–783.

[6] J. H. Fisch, Y. Li, P. C. Kjaer, J. J. Gribble, and T. J. E. Miller, "Pareto-optimal firing angles for switched reluctance motor control," in *Proc. 2nd Int. Conf. Genetic Algorithms Eng. Syst.: Innov. Appl.*, 1997, pp. 90–96.

[7] J. J. Gribble, P. C. Kjaer, and T. J. E. Miller, "Optimal commutation in average torque control of switched reluctance motors," *Proc. Inst. Elect. Eng.—Electr. Power Appl.*, vol. 146, no. 1, pp. 2–10, Jan. 1999.

[8] K. M. Rahman and S. E. Schulz, "High-performance fully digital switched reluctance motor controller for vehicle propulsion," *IEEE Trans. Ind. Appl.*, vol. 38, no. 4, pp. 1062–1071, Jul./Aug. 2002.

[9] Y. Sozer, D. A. Torrey, and E. Mese, "Automatic control of excitation parameters for switched-reluctance motor drives," *IEEE Trans. Power Electron.*, vol. 18, no. 2, pp. 594–603, Mar. 2003.

[10] C. Mademlis and I. Kioskeridis, "Performance optimization in switched reluctance motor drives with online commutation angle control," *IEEE Trans. Energy Convers.*, vol. 18, no. 3, pp. 448–457, Sep. 2003.

[11] P. Niazi, H. A. Toliyat, and A. Goodarzi, "Robust maximum torque per ampere (MTPA) control of PM-assisted SynRM for traction applications," *IEEE Trans. Veh. Technol.*, vol. 56, no. 4, pp. 1538–1545, Jul. 2007.

[12] A. Haddoun, M. E. H. Benbouzid, D. Diallo, R. Abdessemed, J. Ghouili, and K. Srairi, "A loss-minimization DTC scheme for EV induction motors," *IEEE Trans. Veh. Technol.*, vol. 56, no. 1, pp. 81–88, Jan. 2007.

[13] X. D. Xue, K. W. E. Cheng, and S. L. Ho, "A position stepping method for predicting performances of switched reluctance motor drive," *IEEE Trans. Energy Convers.*, vol. 22, no. 4, pp. 839–847, Dec. 2007.

[14] X. D. Xue, K. W. E. Cheng, and S. L. Ho, "Simulation of switched reluctance motor drives using two-dimensional bicubic spline," *IEEE Trans. Energy Convers.*, vol. 17, no. 4, pp. 471–477, Dec. 2002.
[15] X. D. Xue, K. W. E. Cheng, and S. L. Ho, "Online and offline rotary regression analysis of torque estimator for switched reluctance motor drives," *IEEE Trans. Energy Convers.*, vol. 22, no. 4, pp. 810–818, Dec. 2007.
[16] X. D. Xue, K. W. E. Cheng, and S. L. Ho, "A self-training numerical method to calculate the magnetic characteristics for switched reluctance motor drives," *IEEE Trans. Magn.*, vol. 40, no. 2, pp. 734–737, Mar. 2004.

X. D. Xue (M'10) received the B.Eng. degree from Hefei University of Technology, Hefei, China, in 1984, the M.Eng. degree from Tianjin University, Tianjin, China, in 1987, and the Ph.D. degree from the Hong Kong Polytechnic University, Kowloon, Hong Kong, in 2004, all in electrical engineering.

He was a Lecturer and an Associate Professor with the Department of Electrical Engineering, Tianjin University, from 1987 to 2001, where he was engaged in teaching and research. He is currently a Research Fellow with the Department of Electrical Engineering, Hong Kong Polytechnic University. He is the author of over 70 published papers. His research interests include electrical machines, electrical drives, and power electronics. His current research is focused on electric machines and drives applied to electric vehicles and wind-power generations.

K. W. E. Cheng (M'90–SM'06) received the B.Sc. and Ph.D. degrees from the University of Bath, Bath, U.K, in 1987 and 1990, respectively.

He was with Lucas Aerospace, U.K., as a Principal Engineer, where he led a number of power electronics projects before he joined the Hong Kong Polytechnic University, Kowloon, Hong Kong, in 1997, where he is currently a Professor and the Director of the Power Electronics Research Centre. He is the author of over 250 published papers and seven books. His research interests include power electronics, motor drives, electromagnetic interference, electric vehicle, and energy saving.

Dr. Cheng received the Institution of Electrical Engineers Sebastian Z. De Ferranti Premium Award in 1995, the Outstanding Consultancy Award in 2000, the Faculty Merit Award for Best Teaching in 2003 from Hong Kong Polytechnic University, the Faculty Engineering Industrial and Engineering Services Grant Achievement Award in 2006, the Brussels Innova Energy Gold Medal With Mention in 2007, the Consumer Product Design Award in 2008, and the Electric Vehicle Team Faculty Merit Award of the in 2009.

J. K. Lin is currently working toward the Ph.D. degree.

He has been a Research Assistant with the Department of Electrical Engineering, Hong Kong Polytechnic University, Kowloon, Hong Kong. His research interests include power electronics.

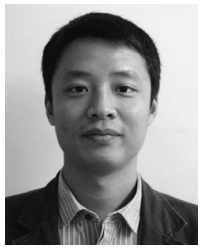

Z. Zhang is currently working toward the Ph.D. degree.

He has been a Research Assistant with the Department of Electrical Engineering, Hong Kong Polytechnic University, Kowloon, Hong Kong. His research interests include power electronics.

K. F. Luk received the degree from Hong Kong Polytechnic University, Kowloon, Hong Kong.

He is a Research Associate with the Department of Electrical Engineering, Hong Kong Polytechnic University. His research interests include power electronics control.

T. W. Ng received the degree from Hong Kong Polytechnic University, Kowloon, Hong Kong.

He is a Research Associate with the Department of Electrical Engineering, Hong Kong Polytechnic University. His research interests include power electronics and charging systems.

N. C. Cheung (S'85–M'91–SM'05) received the B.Sc. degree from the University of London, London, U.K., in 1981, the M.Sc. degree from the University of Hong Kong, Kowloon, Hong Kong, in 1987, and the Ph.D. degree from the University of New South Wales, Kensington, NSW, Australia, in 1996.

He was a Technical Manager with ASM Assembly Automation Ltd., Hong Kong, for two years, working in the areas of intelligent motion control and robotics systems. He has been with the Hong Kong Polytechnic University since 1997, where he is currently with the Department of Electrical Engineering.

Dr. Cheung is a Chartered Engineer in the U.K. and a member of the Institution of Engineering and Technology, U.K.